Worst Frame Backlog Estimation in an Avionics Full-DupleX Switched Ethernet End-System

Yohan Baga*†, Fakhreddine Ghaffari*, Etienne Zante†, Michael Nahmiyace† and David Declercq*
*ETIS, UMR 8051 / ENSEA, University of Cergy-Pontoise, CNRS, F-95000, Cergy-Pontoise, France
Email: (yohan.baga, fakhreddine.ghaffari, david.declercq)@ensea.fr
†ZODIAC AEROSPACE, Zodiac Aero Electric, Zodiac Cockpit and Lighting Systems, Montreuil, France
Email: (etienne.zante, michael.nahmiyace)@zodiacaerospace.com

***Abstract*—With the increase of needs in capability, bandwidth and reliability of modern aeronautical equipment, Avionics Full-Duplex Switched Ethernet (AFDX) network has gained in popularity since its successful implementation in the Airbus A380. As AFDX networkis a deterministic network, frames have to reach the reception End-System (ES) within a limited amount of time: the upper bound of the end-to-end delay. Similarly, a frame arriving at the reception ES has to be processed within a deterministic amount of time to be available to host applications. The duration of frame storage in the ES reception buffer represents a significant part of delays.**

Optimizing the size of the ES reception buffer is then a critical issue, which requires a precise analysis of the Worst Frame Backlog (WFB). This is the issue that we address in this paper. We propose in particular a method to construct the longest sequence of back-to-back frames from a regular reception flow and a simulation tool to estimate the WFB that helps to determine the size of the ES reception buffer for any configuration.

Keywords **–** AFDX Network, End-System Buffer Size, Worst Frame Backlog, Reception Flow, Back-to-back Sequence

I. Introduction

In the next twenty years, the world fleet of civilian airplanes will double arising a challenge for aeronautics industrial stakeholders. Moreover, the future aircraft will embed a huge number of avionics integrated functions both to ensure the safety of the flight and the cabin and cockpit comfort. Thus, the amount of data exchanges and the number of point-to-point connections between equipment will increase significantly, and the embedded communication medium will become a critical issue to satisfy constraints in terms of bandwidth, transmission speed, and reliability.

Embedded networks appear like suitable solutions with the potential to comply with the mentioned requirements and allowing future evolutions. Airbus has proposed an AFDX network based on the proven Ethernet technology. AFDX networks stands for a significant advance compared to its predecessors like ARINC 429 [1] and ARINC 629 [2] which had limited capacities regarding speed (some *Kbps*) and the addressing. In comparison, AFDX networks benefits of the concept of virtual links for multi-point connections and supports a high-speed data transmissions (100 *Mbps*).

ARINC 664 p.7 [3] standardizes the AFDX network and poses requirements to dispose of a real-time, reliable and deterministic communication medium. However, the standard describes the required performances of such network but not the means to achieve them. In particular, determinism is a fundamental property to ensure that data pass through the network in a bounded time interval. System designer has to prove the existence of end-to-end upper bound delays to obtain certification credits from authorities (FAA, EASA).

Proposed in 1991 by Cruz [4] and applied to avionics context in 1998 by Le Boudec [5], *Network Calculus* (NC) is the current method used to compute the End-to-End (ETE) upper bound delays of the AFDX network of commercial aircraft (A380). More recently, *Model Checking* [6] and *Trajectory Approach* (TA) ([7], [8], [9], [10]) have gained in popularity to work out a reliable and less pessimistic ETE computational method than NC. Also, some others works focus on solutions to decrease the ETE delays. In [11] and [12], different scheduling policies have been tested to reduce the transmission jitter while priority of frames based on NC [3] or on TA [13] have been proposed to reduce ETE delay of higher priority frames.

The AFDX network elements (ESs and Switches) are not synchronized with an overall time clock. Therefore, frames may compete for network resources usage such as the non-prehensile queuing First In First Out (FIFO) memories and lead to a sporadic congestion on the physical link. In such scenario, a sequence of back-to-back frames may form at a network node, and it may propagate until the reception ES to constitute a backlog in the reception buffer. A prohibited loss of frames may happen if the size of a FIFO memory of one network node was undersized, with no respect to the worst back-to-back (BTB) frame sequence. Conversely, FIFO memories with an overestimated size guarantee no loss of frames but implies longer ETE delays and additional costs regarding energy and surface.

Some studies have dealt with the estimation of the worst-case backlogs in output ports of switches and have proposed computation methods based on NC [14] or TA [15] for industrial applications. However, little attention has been given to the size of the reception FIFO because it considered without impacts on the ETE network delays (since the delay between the reception of the frame at the ES and the availability of data to the host applications is not taken into account in the computation of ETE delays). However, the ES has to process received frames deterministically and a loss of frames

978-1-5090-2523-7/16/$31.00 ©2016 IEEE

(especially in case of reception of flurries of received frames) may occur in the ES reception buffer under the assumption of the ES can not process received frames at a full bandwidth speed. That is why the size of the ES reception buffer needs to be accurately calculated.

In this paper, we propose a new approach to compute the optimal size of the ES reception buffer based on a given configuration. Two main contributions are described in this work:

- First, for an End-System Reception Configuration Table (ESRCT), we propose an original method to build the longest sequence of BTB frames by adding delays in a periodic reception flow.
- Second, at constant dumping speed, we propose a new simulation tool named Worst Frame Backlog Simulator (WFB-Sim) to emulate the reception stream and to estimate the WFB in the ES reception buffer and consequently, the suitable size of this buffer compliant with the mentioned constrains.

The rest of the paper is organized as follow. Section II introduces a description of the AFDX network. Section III describes the model of the reception flow in order to build the WFB for multiple VLs. Section IV depicts the algorithms of the simulation tool. Section V presents the obtained results for a standard configuration of 50 VLs and the influence of the ESRCT parameters on the WFB computation. Conclusion and future works are presented in section VI.

II. AFDX NETWORK: ARCHITECTURE AND TRAFFIC

The design of AFDX network relies on a topology and a communication protocol so as to meet requirements in terms of real-time transmission and reliability. The following paragraphs present the essential features of an AFDX network and highlight AFDX End-Systems as the interface between the host applications and the AFDX network.

A. Network Architecture

1) Overview: In this study, we deal with an homogeneous AFDX network which offers a deterministic transmission frame service to host applications. The AFDX network is organized around three elements: ESs, switches, and wires. ESs are the source (transmission) and the sink (reception) nodes of the network. The intermediate nodes called switches interconnect ESs via wires. Switches and wires are duplicated and they constitute two parallel sub-networks as specified in the standard ARINC 664 [3] to satisfy reliability demand. With respect to the full duplex feature, wires have to be two differential pairs allowing the simultaneous transmission and reception of frames to avoid collisions and therefore, losses of frames.

Fig. 1 presents an example of AFDX network configuration including 7 ESs $\{ES_i\}$ and 3 switches $\{S_i\}$. Each source ES transmits frames through an output port to one single switch input port. More generally, an ES port is connected to only one switch port resulting in a network in a star topology. Each output port is associated with a buffer ruled by a FIFO policy. The reception ESs receive frames through an input port with a FIFO buffer.

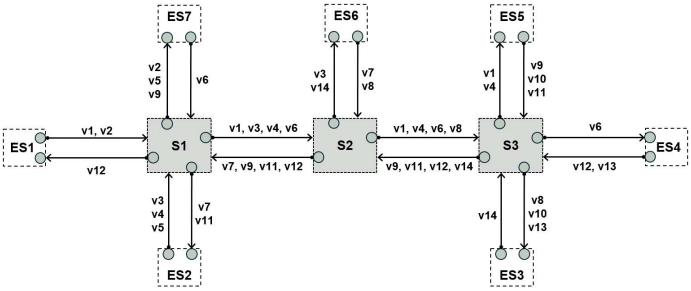

Fig. 1: Example of AFDX Network Configuration.

2) Switch: An AFDX switch ensures the essential services of the network to route transmitted frames correctly until the reception ES. The switch policy is of type store and forward. It receives a frame on the input port, and it then realizes a set of functions (filtering, policing, switching and monitoring functions) before transferring the frame to the suitable output port. The choice of the output port is based on the adequacy between the parameters of the static routing table of the switch and the information of the frame MAC header.

The re-transmission speed of frames is 100 *Mbps* and it can process several frames at the same time. A switch induces a latency on the frame transmission which is included in the ETE delay computation. Thus, latencies in the switch are upper bounded, but they remain variable, depending on the network workload. In particular, concurrent access to a switch output port can lead to an extra latency for the delayed frame even more if the frame passes through several switches before the reception.

3) End-System: The ES provides an interface to allow a reliable and deterministic data exchanges among the software partitions and avionics computer systems. As illustrated in Fig. 2, the ES services are split into three layers. The model of a AFDX ES in layers ties to the Internet TCP/IP protocol. The main difference lies in an intermediate layer (the AFDX Special Features layer) between UDP/IP layers and IEEE 802.3 MAC layer. It comprises two distinct flows as transmission and reception occur in parallel.

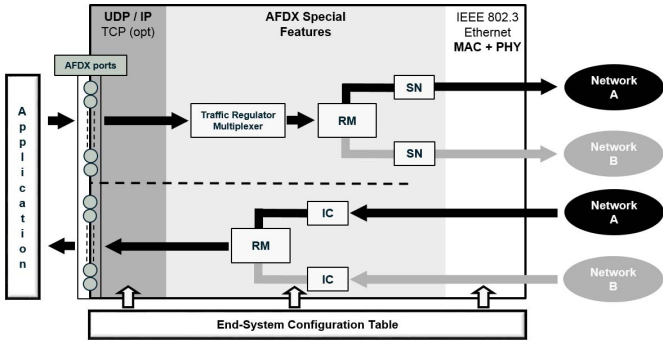

Fig. 2: Architecture of an AFDX End-System.

In transmission, data are generated by software partitions which are units of host applications. They reach the AFDX input ports of source ES (sampling, queuing or SAP). Then, AFDX frames are created by aggregating some data and adding headers and are stored until the date of emission. The traffic regulator periodically sends frames. The period corresponds to a minimum interval of time between two consecutive frames of the same flow. The Redundancy Management (RM) unit duplicates frames and sends them through the A and B sub-networks if a the "'redundant send"' is set. The Sequence Number (SN) unit provides a unique ID to the transmitted frame depending on the considered flow, and it increments this number for successive frames.

In reception, the Integrity Checking (IC) unit controls the SN of received frames. It discards invalid frames. Next, the RM unit accepts and forwards the first valid frame it receives from sub-networks A and B. It follows a series of checks because of the mechanisms of the UDP/IP layers and the resulting data are stored in AFDX ES ports available for the applications.

B. Traffic Modeling

1) Virtual Links: AFDX network enforces the concept of virtual communication channels to exchange data under a real time constraint. A Virtual Link (VL) has one source ES and n reception ESs and it allows unicast, multicast and broadcast transmissions which recall ARINC 429 features. It shares the available bandwidth of the physical link in virtual channels in such a manner that software partitions can instantiate independent communications. Also, the temporal isolation of VLs immunized them against the propagation of a dysfunction. If an abnormal behavior corrupts one VL, the remain VLs, which share the same physical resources, are not affected.

Fig. 1 pictures a set of unicast VLs each one interconnects one source ES to one reception ES. A unidirectional communication path is thus defined as a series of network elements, starting with the source ES and ending with the reception ES. For example, $P_4 = \{ES_2, S_1, S_2, S_3, ES_5\}$ is the path followed by v_4 whose source is ES_2 and sink is ES_5. Multicast transmissions are not considered in our example.

2) Traffic Regulation of Source Flows & End-to-End Delays: The data flow incoming from the source ES is unregulated, and it can lead to an inefficient bandwidth usage and unpredictability of network performances. So the solution standardized in ARINC 664 is to regulate the source of virtual links by defining the Bandwidth Allocation Gap (BAG) as the minimal time slot between two consecutive frames. The BAG is set in the static ESRCT as an essential parameter of a VL in the same way as the maximum frame length L_{max}. Each VL has a single BAG value which ranges in a power of 2 from 0 to 7 i.e. from 1 to 128*ms*. The flow is adjusted depending on the bandwidth needs of the application.

The proof of network determinism strongly relies on the respect of the BAG values under the oversight of the traffic regulator. Thus, the existence of an end-to-end upper bound delay can be measured for each VL, for example, by using a simulation tool [16].

In this paper, we conduct a deep analysis of the arrival flow at the reception ES. We assume that the source flows of the network are well constrained, i.e. all the upper bounds of ETE delays exists.

III. Modeling of the Arrival Flow at a Reception End-System

In this section, we present the hypothesis and the model of frames arrival which lead to computation of the longest sequence of back-to-back frames and the estimation of the Worst Frame Backlog. To do that, we analyze the impacts of temporal perturbations on the flow received at an End-System.

A. Sources of Perturbation impeding a Periodic Reception of Frames

1) Transmission Jitters: The transmission of frames could be periodic on a VL as the traffic regulator shapes frames according to the BAG parameter. In this case, the period of transmission should be equal to the BAG. However, a hosted application usually requires multiple VLs in practical industrial cases to communicate with several other avionic equipment. As the VLs of an ES share a single physical link in transmission, a scheduler multiplexes the concurrent flows coming from the traffic regulator. It manages the flow of VLs with a FIFO policy. Therefore, it may instigate some transmission jitters in the frame delays.

Figure 3 depicts the transmission jitter as a bounded time interval. The maximum value of the transmission jitter is noted J^T_{max}. The source ES regulates the flow on each VL_i in such a way that the first bit of every frame has to appear on the AFDX network before J^T_{max}.

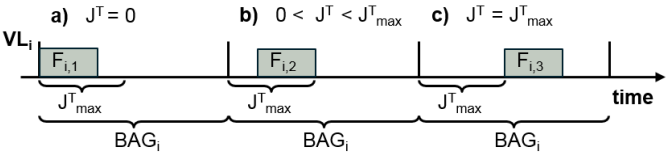

Fig. 3: Effects of the Transmission Jitter on Frames for a VL.

ARINC 664 [3] proposes a range of transmission jitter J^T_{max} for each VL at the output of a source ES:

$$\begin{cases} J^T_{max} \leq 40 + \sum_{i=1}^{\text{Number of VLs}} \frac{(20 + L_{i,max}) \times 8}{C^N} \\ J^T_{max} \leq 500_{\mu s} \end{cases} \quad (1)$$

where :

- J^T_{max} is the maximum allowed value of the transmission jitter, in μs.
- 40 is the minimum technological jitter, in μs.

- 20 is the sum of three fields of the AFDX frame: the preamble ($7\,_{bytes}$), the Start Frame Delimiter ($1\,_{byte}$) and the Inter-Frame Gap ($12\,_{bytes}$), in *bytes*.
- $L_{i,max}$ is the maximal frame length of the i^{th} VL, in *bytes*.
- C^N is the medium bandwidth, in *bits/s*.

Thus, the system integrator disposes of two computational means to decide the value of J^T_{max}. Indeed, J^T_{max} could be lower for small ESRCTs including few virtual links.

The transmission jitter constitutes a source of perturbations regarding the reception periodicity. Perturbations may increase the number of back-to-back frames at the input of the reception ES. For a sake of simplicity, We consider the value $J^T_{max} = 500_{\mu s}$ as a maximum for the transmission jitter to estimate the WFB.

2) Switch Delays: After the transmission by the source ES, frames circulate onto the AFDX network, and they pass through one or several AFDX switches. A switch performs service functions like frame filtering or traffic policing to forward frames to the appropriate physical output port. The achievement of switch operations introduced delays which consist of a technological latency and a frame delay. Switch delays are variable and depend on the workload of the switch at a given time, in particular, the congestion of output ports. Congestions may appear sporadically in a switch and increase the ETE delay of a particular frame.

3) Network Latency Variations: Transmission jitters and variable switch delays result in inconstant ETE delays, even for frames transiting through the same VL. Hence, we can define a global Network Latency Variation (NLV) which is temporally upper bounded as is the ETE delay. The lower bound of the NLV is 0 because two frames can pass through the network under the same latency. As a result, the estimation of the NLV could indicate the degree of perturbation of the received flow and could lead to the measure of the longest back-to-back sequence of frames.

In our approach, we assume the ETE delay known for each VL and we propose a model to assess the NLV. Therefore, we focus on a model of such variations in the following paragraphs.

B. Characterization of Delays for a Non-Periodic Reception

In reception, an ES receives a flow of frames from VLs according to its ESRCT. As previously explained, the NLVs lead to a un-periodic flow. Consequently, frames could arrive in a long back-to-back sequence to the reception ES even if BAG parameters compel the source flows on the AFDX network. This phenomenon leads to backlogs in the FIFO reception buffer of the reception ES.

In order to estimate the WFB, we first have to emulate a flow of frames from a valid ESRCT comprising a list of VL identifiers and their essential parameters (the BAG and the maximum frame length $L_{i,max}$). To do that, we precisely characterize the delays of a frame between the output of the traffic regulator and the reception ES. We consider three scenarios of latencies for the reception of one frame: nominal latencies, minimal latencies, and maximal latencies.

1) Nominal Latencies: The first scenario corresponds to a non-extremal transmission jitter and a non-extremal network delay. It is the most common scenario and the latencies are considered as nominal. This scenario can be expressed by: $\forall\,(\,i\,;\,j\,) \in [\,0\,;\,\infty\,] \times [\,1\,;\,\textit{Number of VLs}\,]$,

$$\begin{cases} J^T_{i,j} & \in &]\,0\,;\,J^T_{max}\,[\\ \theta^N_{i,j} & \in &]\,\theta^N_{i,min}\,;\,\theta^N_{i,max}\,[\end{cases} \tag{2}$$

Fig. 4 illustrates a such scenario for any frame $F_{i,j}$ identified by a unique ID j for a particular VL_i.

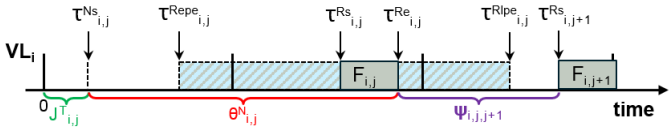

Fig. 4: Nominal Scenario for Reception: Non-Extremal Transmission Jitter and Non-Extremal Network Delay.

After an idle time corresponding to the transmission jitter $J^T_{i,j}$, the AFDX network received the first bit of $F_{i,j}$ at the date $\tau^{Ns}_{i,j}$. Next, the frame $F_{i,j}$ undergoes some network delays $\theta^N_{i,j}$ in accordance with the static path of VL_i (especially the number of passed through switches). If we pose $\Gamma^R_{i,j}$ as the reception latency, we can write :

$$\Gamma^R_{i,j} = J^T_{i,j} + \theta^N_{i,j} \tag{3}$$

In addition, $\tau^{Rs}_{i,j}$ points out the starting reception date, that is to say the date when the first bit of $F_{i,j}$ reaches the input port of the reception ES. Similarly, $\tau^{Re}_{i,j}$ indicates the date when the last bit of $F_{i,j}$ is received. If we assume $\gamma^R_{i,j}$ as the effective duration of the frame reception which depend of the network speed C^N and the maximum frame length $L_{i,max}$ on the VL_i:

$$\begin{array}{lll} \gamma^R_{i,j} & = \tau^{Re}_{i,j} - \tau^{Rs}_{i,j} \\ \gamma^R_{i,j} & = \frac{L_{i,max}}{C^N} \end{array} \tag{4}$$

On the Fig. 4 appears a striped time interval delimited by $\tau^{Repe}_{i,j}$ and $\tau^{Rlpe}_{i,j}$. The existence of his interval is justified by the non-periodic reception of frames because of variable $J^T_{i,j}$ and $\theta^N_{i,j}$. In other words, frames incur different network delays $\theta^N_{i,j}$ and different transmission jitters $J^T_{i,j}$ of each other. So, $\tau^{Re}_{i,j}$ varies depending on frames. Additionally, Eq. 2 precises that whatever j on the same VL_i, $J^T_{i,j}$ and $\theta^N_{i,j}$ are bounded by random values. Consequently, $I^R_{i,j}$ is also bounded and, if we pose $\tau^{Repe}_{i,j}$ as the *earliest* possible date of the total frame $F_{i,j}$ reception and $\tau^{lpf}_{i,j}$ as the *latest* possible date of the total frame $F_{i,j}$ reception:

$$\tau^{Re}_{i,j} \in I^R_{i,j} = \left[\,\tau^{Repe}_{i,j}\,;\,\tau^{Rlpe}_{i,j}\,\right] \tag{5}$$

Last but not least, we propose $\Psi_{i,j,j+1}$ as an inter-frame time variable to measure the local perturbations of periodicity

between two consecutive frames $F_{i,j}$ and $F_{i,j+1}$. From the point of view of the reception ES, it is the idle time between the reception of two consecutive frames on the same VL. The role of $\Psi_{i,j,j+1}$ will be detailed in the next section.

2) Minimal Latencies: The second scenario corresponds to a zero transmission jitter and the minimal network delay that is to say: $\forall\,(\,i\,;\,j\,) \in [\,0\,;\,\infty\,] \times [\,1\,;\,\textit{Number of VLs}\,]$,

$$\begin{cases} J^T_{i,j} &= 0 \\ \theta^N_{i,j} &= \theta^N_{min,i} \end{cases} \tag{6}$$

This scenario can occur if $F_{i,j}$ is sent on the AFDX network immediately after its creation in the source ES and if $F_{i,j}$ meets no congestion during the crossing of the network.

Fig. 5 depicts the reception of a frame $F_{i,j}$ under the minimal latencies. We can deduce from Fig. 5 the minimal

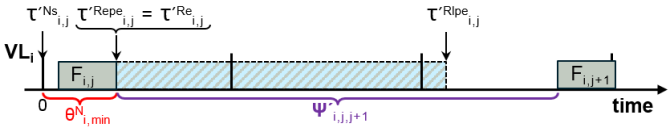

Fig. 5: Extremal Scenario in Reception: Zero Transmission Jitter and Minimal Network Delay.

reception latency $\Gamma^R_{i,min}$ for $F_{i,j}$ which depends only on the VL_i:

$$\Gamma^R_{i,min} = \theta^N_{i,min} \tag{7}$$

In this case, $\tau^{'Re}_{i,j}$ is equal to the *earliest* possible date of the total frame reception $\tau^{'Repe}_{i,j}$

$$\tau^{'Re}_{i,j} = \tau^{'Repe}_{i,j} \tag{8}$$

Besides, it is important to note that the interval moved left compared to the one for nominal latencies. The reason is that $J^T_{i,j}$ behaves like an offset with respect to the lower limit $\tau^{Repe}_{i,j}$ of $I^R_{i,j}$. The immediate consequence is $I^R_{i,j}$ shifts according to the value of $J^T_{i,j}$. With Eq. 8, we can write:

$$\begin{aligned} \tau^{Repe}_{i,j} &= J^T_{i,j} + \tau^{'Repe}_{i,j} \\ \tau^{Repe}_{i,j} &= J^T_{i,j} + \theta^N_{i,min} \end{aligned} \tag{9}$$

So $\tau^{'Repe}_{i,j}$ appears as the lower bound of the variations of $\tau^{Repe}_{i,j}$ and:

$$\tau^{'Repe}_{i,j} = \theta^N_{i,min} \tag{10}$$

3) Maximal Latencies: When the transmission jitter is maximal but also the network delay in accordance with the following conditions: $\forall\,(\,i\,;\,j\,) \in [\,0\,;\,\infty\,] \times [\,1\,;\,\textit{Number of VLs}\,]$,

$$\begin{cases} J^T_{i,j} &= J^T_{max} \\ \theta^N_{i,j} &= \theta^N_{i,max} \end{cases} \tag{11}$$

the worst case frame latency is under consideration. For certification issues, $\theta^N_{i,j}$ has to be upper bounded [3] to guarantee the determinism of the whole network what justifies the existence of $\theta^N_{i,max}$.

Fig. 6 shows the reception of $F_{i,j}$ under maximal latencies. As well for Eq. 7, the maximal reception latency $\Gamma^R_{i,max}$ for

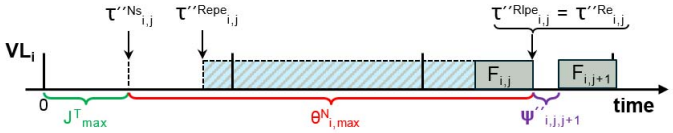

Fig. 6: Extremal Scenario in Reception: Maximal Transmission Jitter and Maximal Network Delay.

$F_{i,j}$ is given by:

$$\Gamma^R_{i,max} = J^T_{max} + \theta^N_{i,max} \tag{12}$$

Therewith, $\tau^{''Re}_{i,j}$ is equal to the *latest* possible date of the total reception $\tau^{''Rlpe}_{i,j}$:

$$\tau^{''Re}_{i,j} = \tau^{''Rlpe}_{i,j} = J^T_{max} + \theta^N_{i,max} \tag{13}$$

Similarly with Eq. 10, $\tau^{''Rlpe}_{i,j}$ appears as the upper bound of the variations of $\tau^{Rlpe}_{i,j}$ and:

$$\tau^{Rlpe}_{i,j} = J^T_{i,j} + \theta^N_{i,max} \tag{14}$$

Extremal cases lead to the conclusion that a frame $F_{i,j}$ can be received at any moment between $\tau^{Repe}_{i,j}$ and $\tau^{Rlpe}_{i,j}$ such as:

$$\begin{cases} \tau^{Repe}_{i,j} &\in \left[\,\theta^N_{i,min}\,;\,J^T_{max} + \theta^N_{i,min}\,\right] \\ \tau^{Rlpe}_{i,j} &\in \left[\,\theta^N_{i,max}\,;\,J^T_{max} + \theta^N_{i,max}\,\right] \end{cases} \tag{15}$$

C. Consequences of a Non-Periodic Flow on the Reception End-System

In this section, we focus on to the variations of the inter-frame time duration and its consequences on the frame stream received at the reception ES.

1) One Single VL: $\Psi_{i,j,j+1}$ allows to locally measure the inter-frame time duration between $F_{i,j}$ and $F_{i,j+1}$ of the VL_i. As illustrated on the Fig. 7, $\Psi_{i,j,j+1}$ reaches different values which can be regrouped in three categories.

Fig. 7a shows the case when the NLVs are close from one frame to each other. This case is a nominal reception and it presents no sequence of back-to-back frames, so the backlog at the reception ES is non-existent.

Fig. 7b is the scenario when the frame $F_{i,j+2}$ has undergone a higher ETE delay than the previous frame $F_{i,j+1}$ when it passed through the AFDX network. For instance, the frame $F_{i,j+2}$ could have met a congestion in a switch which did not exist when the frame $F_{i,j+1}$ has passed through the same switch some milliseconds before. As the latency $\Psi'_{i,j+1,j+2}$

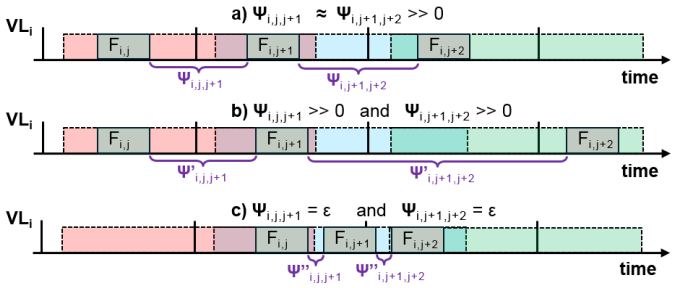

Fig. 7: Variations of the inter-frame time Ψ_i for Three Consecutive Frames of one single VL_i.

increases compared to $\Psi^{'}_{i,j,j+1}$, no backlog will hit the reception ES as it will have more time to process the frame $F_{i,j+1}$.

Finally, Fig. 7c depicts the scenario driving to a sequence of BTB frames. $\Psi^{''}_{i,j,j+1}$ and $\Psi^{''}_{i,j+1,j+2}$ have low values such as:

$$\Psi^{''}_{i,j,j+1} \approx \Psi^{''}_{i,j+1,j+2} \approx \varepsilon \tag{16}$$

and ε is the shortest time duration between two consecutive frames of VL_i:

$$\varepsilon = \frac{20_{\text{bytes}}}{C^N} \tag{17}$$

This scenario can occur if the time duration between the latest possible date of the total frame $F_{i,j}$ reception $\tau^{Rlpe}_{i,j}$ and the earliest possible date of the total frame $F_{i,j+1}$ reception $\tau^{Repe}_{i,j+1}$ is less than ε:

$$\tau^{Repe}_{i,j+1} - \tau^{Rlpe}_{i,j} \leq \varepsilon \tag{18}$$

Moreover, in the general case, $\Psi_{i,j,j+1}$ is upper bounded according to Eq. 15 under the assumption that frames are transmitted at BAG_i such as:

$$\begin{cases} \Psi_{i,j,j+1,max} = & \tau^{Rlpe}_{i,j+1,max} - \tau^{Repe}_{i,j,min} \\ \Psi_{i,j,j+1,max} = & J^T_{max} + \theta^N_{i,max} + BAG_i - \theta^N_{i,min} \end{cases} \tag{19}$$

2) Multiple VLs: We presented our frame reception model for one single VL and we took into account the non-periodicity to mathematically express a back-to-back frame reception. Now, we intend to make an extension of the previous model to n VLs in order to get closer to a real ESRCT.

To do that, we start by representing the reception flow between the last switch and the reception ES without any NLVs. It means that frames are periodically received and thus, the reception flow is also periodic.

On the Fig. 8 a such periodic reception flow is represented for a reduced configuration comprising 4 VLs. We assume the source ESs start to transmit in such a way that the Longest Periodic Sequence (LPS) of BTB frames (equal to the number of VLs) periodically appears in the last physical link. It is not trivial that this scenario corresponds to a synchronous sending of frames on the AFDX network since a single ES can be the source of several VLs. From Eq. 17, a reception of BTB frames implies that the duration ε separates two consecutive frames in the physical link.

Under the hypothesis made, the LPS lasts λ^{Rp}_{max} and repeats each BAG_{max} which is defined as the highest BAG value of the ESRCT such as λ^{Rp}_{max} is given by:

$$\lambda^{Rp}_{max} = \sum_{i=1}^{\text{Number of VLs}} \frac{(20 + L_{max}) \times 8}{C^N} \tag{20}$$

Then, we identify the nearby frames which could increase the LPS with the effects of the NLVs. Thus, we represent on the Fig. 8 two time windows built: the first one φ^b_{max} defined before the first frame of the LPS and the second one φ^a_{max} defined after the last frame of the LPS. φ^b_{max} and φ^a_{max} are equal and represent the maximal NLV. We make the assumption that the maximal NLV is the same for all VLs such as:

$$\begin{array}{rcccl} \varphi^b_{max} & = & \varphi^a_{max} & = & J^T_{max} + \theta^N_{max} - \theta^N_{min} \\ \varphi^b_{max} & = & \varphi^a_{max} & \approx & \theta^N_{max} - \theta^N_{min} \end{array} \tag{21}$$

At this point, it is necessary to define the Longest Non-Periodic Sequence (LNPS) of BTB frames which is formed by the LPS plus the nearby frames the which could increase the LPS with the effects of the NLVs. From Eq. 21 and Eq. 19, we can infer conditions for a frame to be appended to the LNPS.

- For each VL, if we consider the frame $j+1$ belonging to the LPS, the frame j can be included in the LNPS if: $\varphi^b_{max} > \Psi_{i,j,j+1,max}$.
- For each VL, if we consider the frame $j+1$ belonging to the LPS, the frame $j+2$ can be included in the LNPS if: $\varphi^a_{max} > \Psi_{i,j+1,j+2,max}$.

Moreover, the frames received in φ^b_{max} have negative indexes (-1 and -2) and the older frames outside φ^b_{max} have n in index such as: $-n << -2$. Identically, the frames received in φ^a_{max} have positive indexes (1, 2 and 3) and next frames outside φ^b_{max} have m in dex such as: $m >> 3$. The frames belonging to the LPS have index 0.

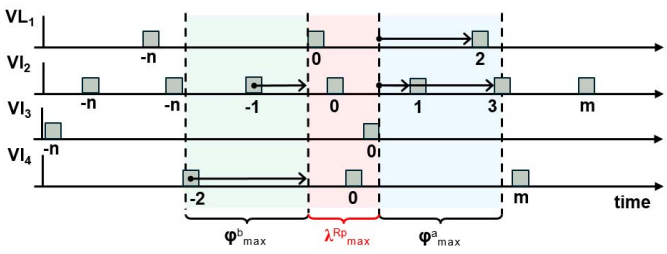

Fig. 8: Identification of the LPS with a Duration of λ^{Rp}_{max} and the Time Windows φ_{max} on a Reduced ESRCT of 4 VLs.

The frame index -1 received in the time window φ^b_{max} could undergo NLVs and could bring closer to the first frame of the LPS. If these two frames were separated only by an ε, the frame index -1 would be part of the LNPS.

For the time window φ^a_{max}, the frames index 1, 2 and 3 could be added to the LNPS. However, if the LPS was delayed, it would be reasonable to assume that some frames of φ^b_{max} could not anymore be part of the LNPS.

To the sake of simplicity, we make a pessimist assumption: all frames in times windows φ^b_{max} and φ^a_{max} can be included in the LNPS. Thus, if we pose λ^{Rnp}_{max} as the duration of the LNPS, we can write:

$$\lambda^{Rnp}_{max} = \lambda^{Rp}_{max} + \sum_{\substack{Frames \in \Psi^b_{max} \\ Frames \in \Psi^a_{max}}} \frac{(20 + L_{max}) \times 8}{C^N} \qquad (22)$$

To sum up, we presented a model to estimate the LNPS for multiple VLs from a periodic reception flow in which we inject NLVs to create the LNPS. As the calculation of the WFB comes quickly with the LNPS, only the simulation results will be presented in this paper.

IV. Algorithmic of the Simulation Tool

To enforce our theoretical model, we propose an overview of algorithms implemented in WFB-Sim and the calculation procedure.

The goal is to compute the WFB from the LNPS and to deduce the optimal size of the ES reception buffer. WFB-Sim calculates the LNPS from any set of ESRCT parameters. The configuration file contains ESRCT parameters which mean some virtual links associated with their BAG and the maximal allowed frame length.

Firstly, WFB-Sim downloads the ESRCT parameters, and it uses them to allocate the required memory to store results by computing the length of the simulation in a number of frames. To do that, WFB-Sim calculates the Periodic Pattern (PP). It is a constant number of frames as the NLVs are set to 0. Thus, the received flow is periodic, and the PP is infinitely repeated with a period equal to the maximal BAG among ESRCT parameters. However, the analysis can be limited to some PPs which depends on φ_{max} (Eq. 21). The user sets the value of φ_{max} as the maximal NLV. Therefore, WFB-Sim can compute the number of PPs required for the analysis and it reserves the needed memory space.

Then, WFB-Sim generates the received flow by processing all the starting and the ending reception dates of frames. It detects the number of LPSs which is equal to the number of received PPs and records their features. Features of the LPS constitute a reference to estimate the impact of perturbations on the periodic flow at the ES.

The computation of the LNPS affects frames arriving in the interval $[\,\varphi^b_{max}\,;\,\varphi^a_{max}\,]$ around any LPS. In order to complete the construction of the LNPS, the central LPS is targeted to undergo perturbations. Thus, an index is attributed to every frame: 0 for frames of the LPS, a positive index for frames arriving after the last frame of the LPS, and a negative index for frames arriving before the first frame of the LPS.

The next algorithm computes the new arrival dates of frames belonging to $[\varphi^b_{max}; \varphi^a_{max}]$. The LNPS is created and WFB-Sim characterizes the LNPS, in particular the total duration λ^{Rnp}_{max} (Eq. 22).

The computation of the WFB in the reception buffer requires the knowledge of the output throughput of the reception buffer and the delay between the reception of the last bit of a frame in the reception buffer and the start date of the reading of this frame. So, WFB-Sim processes the output flow of the ES towards the software partitions. The frame backlog is obtained as the difference between these two flows and the WFB as the maximal value of the frame backlog during the reception of the LNPS.

V. Application on an Industrial Example

We present the results of the LNPS and the WFB estimation obtained for an industrial End-System Configuration Table and the influence of ESRCT parameters variations on the WFB in the reception buffer of an End-System.

A. A realistic Configuration of an End-System in Reception

We use a standard ES configuration to realize the simulation. It comprises 50 VLs in reception knowing that some ESs can manage a maximum of 512 VLs in reception as the ES solution proposed by TTTech [17].

Fig. 9 indicates the distribution of ESRCT parameters chosen for the VLs. Fig. 9a shows the distribution of VLs among BAG values. High values of BAG are privileged because it corresponds to a more realistic configuration of an AFDX network. In our example, more than 70% of BAG values are dispatched between 32, 64 and 128*ms*. Moreover, few VLs require a BAG of 2 or 4*ms* (only 5) and none a BAG of 1*ms* as this extremal value is too rarely used in industrial applications.

Concerning the distribution of the maximal frame length for each VL, Fig. 9b points out that short frames (less than 300*bytes*) represent approximately 80% of the whole configuration. In the same way, medium frames (between 300 and 900*bytes*) represent about 8% of total maximal length. The large frames (more than 900*bytes*) are quite rare in AFDX network configurations but we take them in our approach.

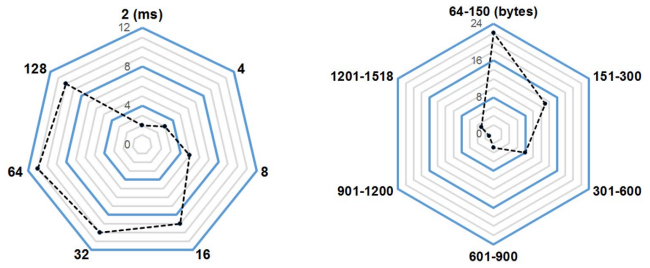

(a) Distribution of VLs among BAGs.

(b) Distribution of VLs among Frame Lengths.

Fig. 9: ESRCT Parameters Distribution for the Configuration of 50 VLs under study.

B. Simulation Results

1) LNPS: To process the LNPS, WFB-Sim needs to the value of Ψ_{max}. Therefore, we set the maximal NVL Ψ_{max} to 10_{ms} for all VLs. This value is chosen to take into account the fact that frames can pass through several switches and undergo important NLVs.

Tab. I summarizes the results provided by WFB-Sim for the presented configuration of 50 VLs.

TABLE I: Features of the Periodic and Non-Periodic Longest Sequences of BTB frames for an ESRCT of 50 VLs.

Periodic	Number of Frames in the PP	346
	Length of the LPS	50
Non-Periodic	Length of the LNPS	76
	Duration of the LNPS, (μs)	19 296
	Amount of Received Bytes (MAC Frames), $(bytes)$	22 650

As expected, the LPS equals the number of VLs as the speed of transmission of the network is sufficient to avoid a larger sequence of BTB frames given the fact that the number of VLs is relatively small.

Moreover, the injected perturbations add 26 frames to the LPS and lead to an LNPS of 76 frames for a total duration of $19.296\mu s$. Last but not least, the amount of received bytes sums all the maximal lengths of frames of the LNPS. It is to highlight that we consider MAC frames and not AFDX frames. It means the preamble, the SFD, and the IFG are removed before the storage of frames.

2) WFB: The LNPS allows the calculation of the input flow of the reception buffer. It is a step function with upward slopes and constant steps alternately which correspond to a reception state at wire speed and an idle state respectively. For the output flow, we assume that the output throughput is the same as the input throughput. In addition, we set the delay to read a received frame to $10\mu s$.

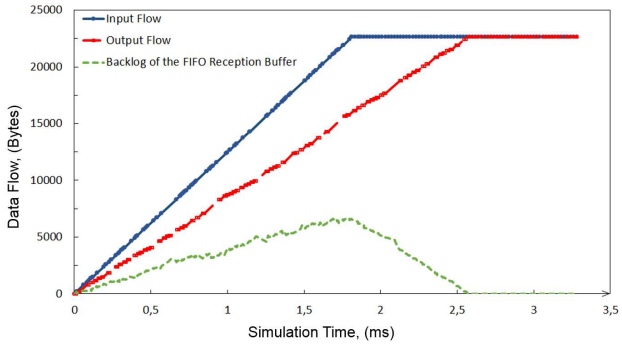

Fig. 10: Estimation of the WFB for the LNPS applied to an ESRCT of 50 VLs.

Fig. 10 shows the input and output flows of the FIFO reception buffer of the reception ES for the LNPS. The reception starts at the date 0 and finishes at $1.8104\mu s$ for the reception of 22 650_{bytes}. The reception ES empties its reception buffer by reading the received frames. The buffer is empty at $2.5504\mu s$. The backlog is represented as the difference of the two previous curves. On Fig. 10, a maximum appears at $1.7932\mu s$ and the resulting WFB is of 6 670_{bytes}. Therefore, the size of the ES reception buffer has to be at least of a size 6 670_{bytes} plus a margin to guarantee no loss of frames.

C. Influence of ESRCT Parameters

In this section, we analyze the influence of ESRCT parameters on the estimation of the WFB in order to evaluate the importance of each type of parameters in the final result.

1) Number of VLs: Fig. 11 presents the results of the LNPS and the WFB for a range of VLs from 5 to 100. We assume that the other parameters are set as a manner to respect the proportions mentioned in section V-A. The size of the WFB is indicated on the left axis and the duration of the LNPS can be measured with the right axis.

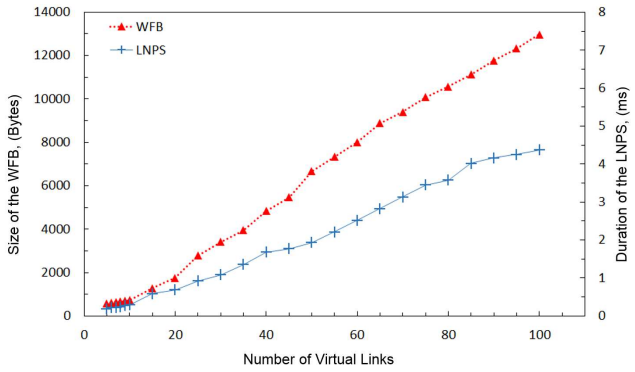

Fig. 11: Influence of the Number of VLs on the Estimation of the LNPS and the WFB.

The results are linear which is not surprising. Each time a VL is added to the ESRCT, the LPS increases of at least one frame. Therefore, the LNPS increases in turn and so the WFB.

Fig. 12 represents the impact of an increase of the number of VLs on the number of frames of the LNPS and on the PP.

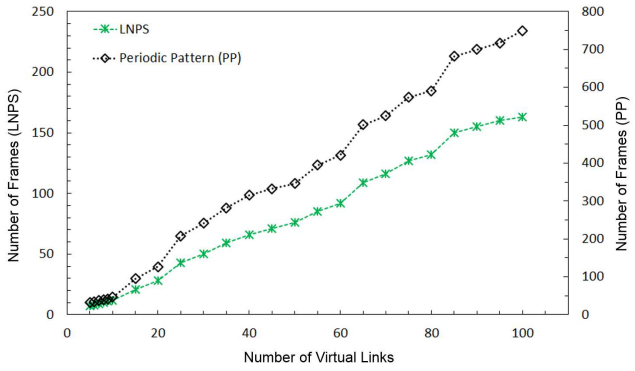

Fig. 12: Evolution of LNPS & PP with the Increase of the Number of VLs.

These results confirm what the intuition suggests that is an increase of the number of VLs of the ESRCT leads to an increase of the WFB and therefore, to the fact that the designer has to consider a larger FIFO reception buffer.

2) BAG: Evaluating the influence of the BAG on the WFB in a reception ES is a difficult task since we first have to choose an adequate metric to measure the variations of the BAG of the entire ESRCT. The average BAG value of all VLs seems a good candidate to assess the BAG variations as shown in Fig. 13. It presents the values of the LNPS, and the WFB globally decrease with the increase of the average BAG. However, the first WFBs and LNPSs slightly increase for an average BAG close to $35\mu s$ because the BAG values are more and more small, and so, the distribution of BAG values is more restricted.

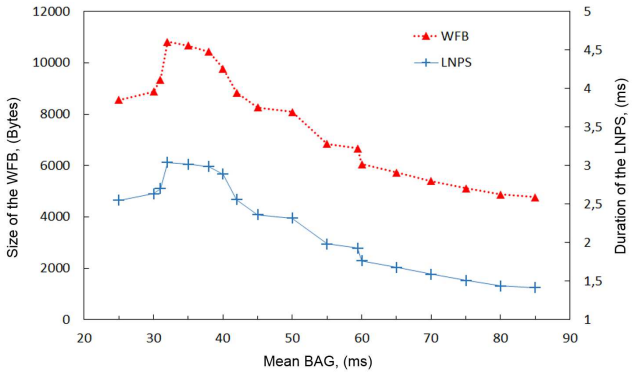

Fig. 13: Influence of the Mean BAG on the Estimation of the LNPS and the WFB.

The size of the WFB stabilizes after an average BAG of $60\mu s$. That means that the high is the average BAG, the more is it likely that frames on a same VL are separated by a duration such as for two consecutive frames j and $j+1$ (with $j+1$ belonging to the LPS), the condition $\varphi^{b}_{max} > \Psi_{i,j,j+1,max}$ is not respected. Therefore, fewer frames can be added to the LNPS.

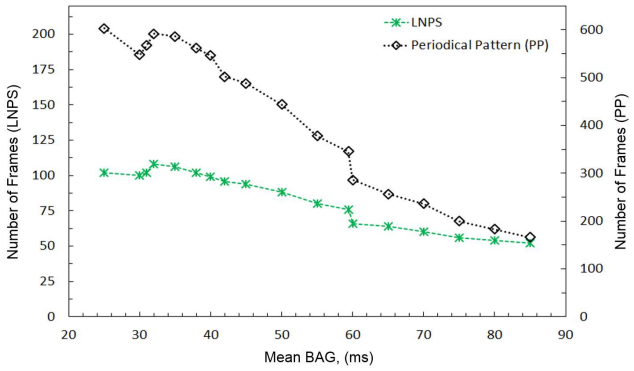

Fig. 14: Evolution of LNPS & PP with the Increase of the Average BAG.

Fig. 14 illustrates the influence of the average BAG on the number of frames of the LNPS and the PP. We can see a decrease of the LNPS and the PP for an average BAG close to $35\mu s$ which corroborates the previous results.

3) Maximal Length of Frames: Finally, we focus on the influence of maximal frame lengths on the calculation of the WFB. Each VL presents a length parameter which is the maximal frame length allowed for all frames transiting on the VL under consideration. As for the BAG, we use of the average to evaluate the variations of maximal frame lengths of the ESRCT of 50 VLs given as a reference. The studied interval starts from an average of 200_{bytes} to an average of 500_{bytes}.

Fig. 15 shows the size of the WFB and the LNPS in function of the average of maximal frame lengths. The reference ESRCT has an average of the maximal frame lengths of 310.2_{bytes}. It results in a WFB of 6 670_{bytes} and a duration of the LNPS of $1.932\mu s$.

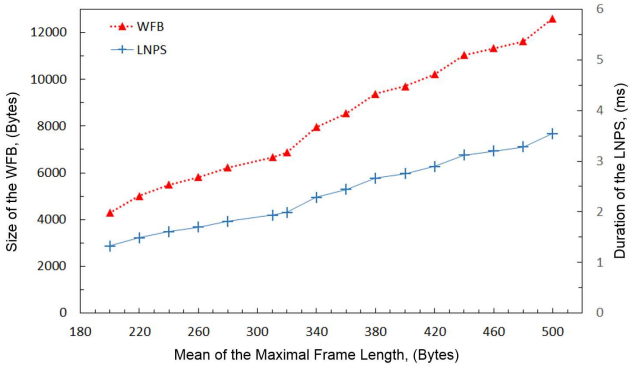

Fig. 15: Influence of the Mean of the Maximal Length of Frames on the Estimation of the WFB.

When the average of maximal frame lengths increases, the LNPS and the WFB increase linearly. For example, the WFB is of 12 614_{bytes} for an average of maximal frame lengths of 500bytes.

Moreover, the maximal frame length does not influence the PP and the LNPS regarding the number of frames since these figures stay constant both for the PP and the LNPS.

VI. Conclusion and Perspectives

An optimal dimensioning of the FIFO reception buffer is a critical issue to improve the performance of an End-System and to comply with the avionic constraints.

In this paper, we introduced an original model to estimate the Worst Frame Backlog (WFB) for any ESRCT considering a periodic flow perturbed by sources of un-periodicity like transmission jitters and switch delays. A precise characterization of these variable delays allows constructing the longest un-periodic sequence (LNPS) of back-to-back frames. The LNPS is considered as the worst scenario of back-to-back frame reception and it is used to compute the WFB. We point out the direct link between the WFB and the size of the ES reception buffer.

From our model, we designed a simulation tool (WFB-Sim) which gives promising results for a standard ESRCT. We highlight the influence of the number of VLs, the average BAG and the average of maximal frame lengths on the WFB calculation. Among these three parameters, we observe that the increase in the number of VLs has a significant impact on the WFB.

Future works will be led to improve the algorithms for simulation by considering delay variations on independent VLs since the VLs passes through a different number of switches according to their source ES. Moreover, complement works will focus on the potential permutations of the frames in reception and the impact on the calculation of the WFB.

REFERENCES

[1] Aeronautical Radio Inc., *ARINC429: Mark 33 Digital Information Transfer System (DITS), Part 1: Functional Description, Electrical Interfaces, Labels Assignments and Words Formats*, 1995.

[2] Aeronautical Radio Inc., *ARINC629: Avionic Data Bus Standard*, 1995.

[3] Aeronautical Radio Inc., *ARINC664: Aircraft Data Network, Part 7: Avionics Full-Duplex Switched Ethernet Network, 2009*, 2008.

[4] R. L. Cruz, "A calculus for network delay," *IEEE Transactions on Information Theory*, vol. 37, pp. 114–131, January 1991.

[5] J. Y. L. Boudec, "Application of network calculus to guaranteed service networks," *IEEE Transactions on Information Theory*, vol. 113, pp. 1087–1096, 1998.

[6] J. E. M. Adnan, J. L. Scharbarg and C. Fraboul, "Model for worst case delay analysis of an afdx network using timed automata," *Emerging Technologies and Factory Automation (ETFA), 2010 IEEE Conference on*, 2010.

[7] J. L. S. H. Bauer and C. Fraboul, "Applying and optimizing trajectory approach for performance evaluation of afdx avionics network," *IEEE Conference on Emerging Technologies and Factory Automation*, 2009.

[8] H. B. G. Kemayo, F. Ridouard and P. Richard, "Optimistic problems in the trajectory approach in fifo context," *IEEE 18th Conference on Emerging Technologies and Factory Automation (ETFA)*, 2013.

[9] H. B. G. Kemayo, F. Ridouard and P. Richard, "Optimism due to serialization in the trajectory approach for switched ethernet networks.," *Proc. of Int. Conf. on Junior Researcher Workshop on Real-Time Computing (JRWRTC)*, pp. 13–16, 2013.

[10] O. C. X. Li and L. George, "The trajectory approach for afdx fifo networks revisited and corrected," *IEEE 20th International Conference on Embedded and Real-Time Computing Systems and Applications*, 2014.

[11] K. L. C. Suthaputchakun and Z. Sun, "Impact of end system scheduling policies on afdx performance in avionic on-board data network," *Advanced Informatics: Concepts, Theory and Applications (ICAICTA), 2015 2nd International Conference on*, pp. 1–6, Aug 2015.

[12] S. Gurjar and B. Lakshmi, "Optimal scheduling policy for jitter control in afdx end-system," *Recent Advances and Innovations in Engineering (ICRAIE)*, 2014.

[13] J. L. S. T. Hamza and C. Fraboul, "Priority assignment on an avionics switched ethernet network (qos afdx)," *10th IEEE Workshop on Factory Communication Systems (WFCS)*, pp. 1–8, May 2014.

[14] W. X. W. Zhitao, L. Tangqi and H. Ning, "The buffer size assignment of afdx based on network calculus," *Reliability, Maintainability and Safety (ICRMS)*, 2011.

[15] G. F. R. Coelho and J. L. Scharbarg, "Dimensioning buffers for afdx networks with multiple priorities virtual links," *Digital Avionics Systems Conference (DASC), 2015 IEEE/AIAA 34th*, 2015.

[16] H. Charara and C. Fraboul, "Modelling and simulation of an avionics full duplex switched ethernet," *Telecommunications, 2005. advanced industrial conference on telecommunications/service assurance with partial and intermittent resources conference/e-learning on telecommunications workshop. aict/sapir/elete 2005. proceedings*, pp. 207–212, July 2005.

[17] TTTech, *TTTech TTE End-System A664 T datasheet*, 2015.